



# Using LiDAR and GEOBIA for automated extraction of eighteenth–late nineteenth century relict charcoal hearths in southern New England

Chandi Witharana, William B. Ouimet & Katharine M. Johnson

To cite this article: Chandi Witharana, William B. Ouimet & Katharine M. Johnson (2018) Using LiDAR and GEOBIA for automated extraction of eighteenth–late nineteenth century relict charcoal hearths in southern New England, GIScience & Remote Sensing, 55:2, 183-204, DOI: 10.1080/15481603.2018.1431356

To link to this article: <https://doi.org/10.1080/15481603.2018.1431356>



Accepted author version posted online: 22 Jan 2018.  
Published online: 05 Feb 2018.



Submit your article to this journal [↗](#)



Article views: 96



View related articles [↗](#)




View Crossmark data [↗](#)



Citing articles: 1 View citing articles [↗](#)



## Using LiDAR and GEOBIA for automated extraction of eighteenth–late nineteenth century relict charcoal hearths in southern New England

Chandi Witharana<sup>\*a</sup>, William B. Ouimet<sup>b</sup> and Katharine M. Johnson <sup>b,c</sup>

<sup>a</sup>*Department of Natural Resources and the Environment, Eversource Energy Center, University of Connecticut, Storrs, CT, USA;* <sup>b</sup>*Department of Geography and Center for Integrative Geosciences, University of Connecticut, Storrs, CT, USA;* <sup>c</sup>*Earth Resources Technology, Inc., NOAA National Centers for Environmental Information, Asheville, NC 28801, USA*

(Received 28 August 2017; accepted 17 January 2018)

Increasing availability and advancements of aerial Light Detection and Ranging (LiDAR) data have radically been shifting the way archeological surveys are performed. Unlike optical remote sensing imagery, LiDAR pulses travel through small gaps in dense tree canopies enabling archeologists to discover “hidden” past settlements and anthropogenic landscape features. While LiDAR has been increasingly adopted in archeological studies worldwide, its full potential is still being explored in the United States. Furthermore, while hand-digitizing features in remote-sensing datasets remain a valuable method for archeological surveys, it is often time- and labor intensive. The central objective of this research is to develop a geographic object-based image analysis-driven methodological framework linking low-level features and domain knowledge to automatically extract targets of interest from LiDAR-based digital terrain models (DTMs) and to closely examine the degree of interoperability of knowledge-based rulesets across different study sites focusing on the same semantic class. We apply this framework in southern New England, a geographic region in the northeastern United States where numerous seventeenth-century to early twentieth-century features such as relict charcoal hearths (RCHs), stone walls, and building foundations lie abandoned in densely forested terrain. Focusing on RCHs in this study, our results show promising agreement between manual and automated detection of these features. Overall, we show that the use of LiDAR data augmented with object-based classification workflows provides valuable baseline data for future archeological study and reconstruction of land-use/land-cover change over the past 300 years.

**Keywords:** LiDAR; GEOBIA; New England; relict charcoal hearths; historical archaeology

### 1. Introduction

LiDAR has recently become an essential tool in archeological studies on a global scale, particularly in areas with densely forested landscapes (Chase et al. 2011; Crow et al. 2007; Doneus et al. 2008; Evans et al. 2013; Gallagher and Josephs 2008; Howey et al. 2016; Johnson and Ouimet 2014; Lasaponara and Masini 2009; Millard et al. 2009; Opitz et al. 2015; Randall 2014). Its use in the United States has grown markedly in the past few years, and the increasing availability of high-resolution data has begun to revolutionize

---

\*Corresponding author. Email: [chandi.witharana@uconn.edu](mailto:chandi.witharana@uconn.edu)

For submission to the special issue of GIScience and Remote Sensing “Remote Sensing of Our Changing Landscapes with Geographic Object-based Image Analysis.”

traditional methods of time-intensive field surveys to identify cultural landscape features (Prufer and Thompson 2016). Ongoing development of a variety of visualization techniques has allowed users to identify increasing types and numbers of archeological landscape features as well (Bennett et al. 2012; Challis, Forlin, and Kinney 2011; Hesse 2010; Kokalj, Zakšek, and Oštir 2011; McCoy, Asner, and Graves 2011). Manual digitization of features coupled with field validation has been a common method of mapping and analysis; however, many studies have also begun to benefit from preliminary automated extraction methods for specific identified features (Cowley 2012).

Various methods have been developed to automatically extract, classify, or characterize various objects (particularly in forestry) as well as cultural features from the surrounding landscape surveyed with LiDAR (Antonarakis, Richards, and Brasington 2008; Blanchard, Jakubowski, and Kelly 2011; Chen and Hay 2011; Cowley 2012; Luo et al. 2014; Smits et al. 2012). Some techniques may be difficult to broadly apply to all study regions due to the differences in landscape type, vegetation, slope, and topography. In terms of archeology, many of these currently published methods extract spherical or round archeological landscape features such as mound structures, pit features, as well as charcoal hearths (Howey et al. 2016; Schneider et al. 2015; Trier, Zortea, and Tønning 2015; Trier, Larsen, and Solberg 2009; Trier and Pilø 2012). These methods generally use supervised classification or delineation techniques coupled with imagery to process the data. While objects such as individual trees and associated forest structure and buildings have been identified and extracted using geographic object-based image analysis (GEOBIA) (e.g., Blaschke et al. 2014; Chen and Hay 2011), only a few studies (e.g., Verhagen and Drăguț 2012) have utilized GEOBIA to extract archeological features of interest from LiDAR data.

Compared to traditional per-pixel based methods, GEOBIA has proven to be one of the most powerful innovations in modern remote sensing for classification and analysis of very high spatial resolution imagery as well as harmonizing other remote-sensing data products such as dense point clouds. The central objective of this research is to develop a GEOBIA-driven methodological framework linking low-level motifs and domain knowledge (Gu et al. 2017) to extract archeological targets of interest from LiDAR-based digital terrain models (DTMs) and to closely examine the degree of interoperability of knowledge-based rulesets across different study sites focusing on the same semantic class.

The GEOBIA-driven methodological framework presented in this study is applied in southern New England, a geographic region in the northeastern United States. Southern New England harbors a unique historical and geomorphological landscape that preserves a dramatic transformation of widespread seventeenth to early twentieth-century deforestation and agriculture followed by abandonment and reforestation. Publicly available LiDAR point clouds and derivative DTMs have revolutionized the ability to identify abandoned archeological features below the forest canopy in this region (Johnson and Ouimet 2014). Notable features include stone walls and building foundations, which indicate settlement areas and fields used for agriculture and pasture, and relict charcoal hearths (RCHs), which are relatively flat, circular/elliptical platforms built for facilitating the production of charcoal from forest hardwoods and softwoods (Johnson, Ouimet, and Raslan 2015; Raab et al. 2017). The particular focus of this study is on the combination of LiDAR and GEOBIA for semi-/full-automated detection of RCHs. The overall goals of this study are to (1) present a conceptual framework and implementation of GEOBIA for detection of RCHs in southern New England; (2) report on image segmentation, rule-set transferability, and classification accuracy assessment; and (3) discuss the potential of GEOBIA in semi-/full-automated detection, transferability of object-based rulesets,

opportunities for migrating the proposed conceptual framework to an operational context, and implications for historical archeology studies in the region and in other areas where similar types of features are found.

## 2. Materials and methods

### 2.1. Study area and remote sensing data

Our two study sites are in the northwestern corner of the state of Connecticut, which lies in the northeastern United States (Figure 1). This region is generally characterized by undulating topography dominated with dense tree cover composed of northern hardwoods and deciduous forest (Foster et al. 2008). Each of the two study sites covers 10 km<sup>2</sup> and contains nearly 1000 RCHs (Figure 2). These sites were previously mapped as part of a broader investigation of seventeenth to early twentieth century archeological features preserved below the forest canopy throughout areas of Connecticut (Johnson and Ouimet 2014; Johnson, Ouimet, and Raslan 2015; Johnson and Ouimet 2016), but in each case, identification and mapping of archeological features (including RCHs) were done by hand-digitization.

In some locations of northwestern Connecticut, hand-digitization found there to be >100 charcoal hearths per km<sup>2</sup> (Johnson, Ouimet, and Raslan 2015). The reason for the high concentration of RCHs in northwestern Connecticut is because iron mining and subsequent processing was a primary industry in the late eighteenth to late nineteenth century. Prior to the arrival of coal from other regions of the eastern United States beginning in the late nineteenth century, charcoal was produced through local deforestation near RCH sites and was the primary source of fuel for iron furnaces. Recent field

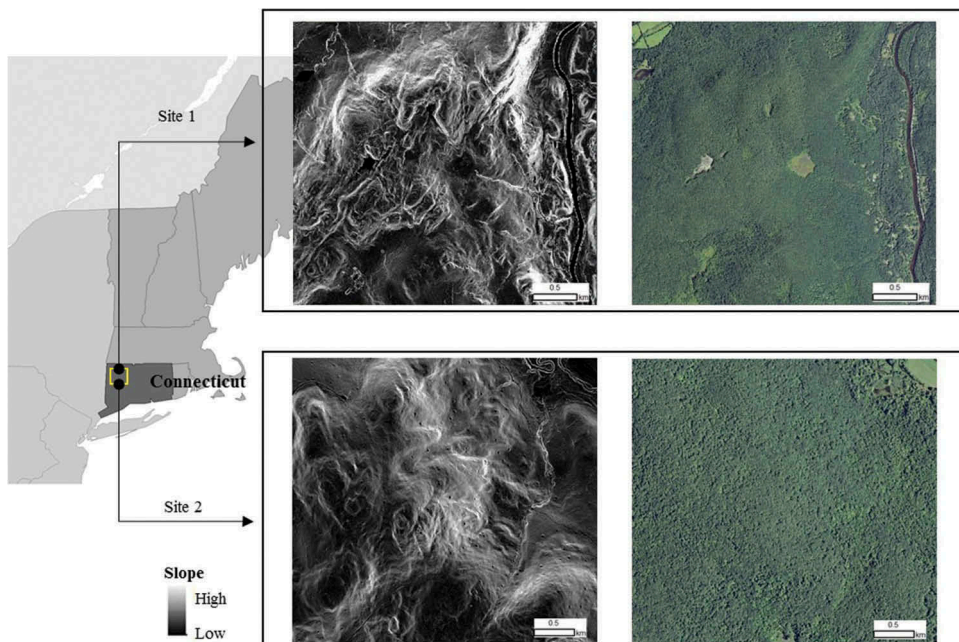


Figure 1. Study sites with slope (left, derived from a 2011 ground-classified LiDAR DTM) and aerial imagery (right, acquired in Summer 2012).

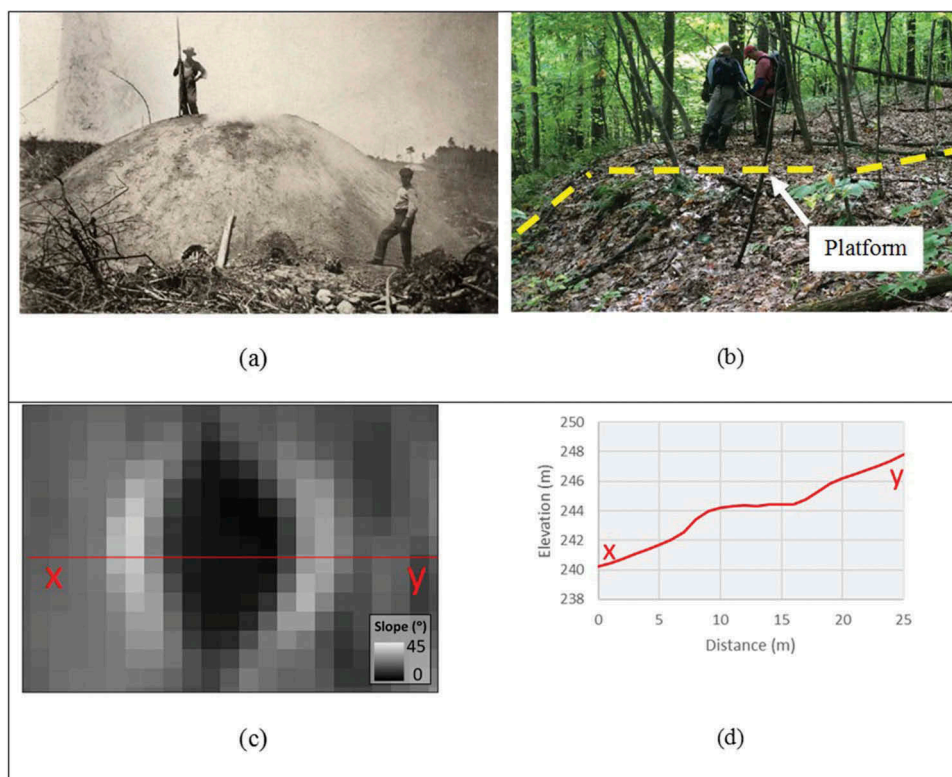


Figure 2. Historical photo showing actual charcoal hearth (RCH) (courtesy Cornwall Historical Society) (a), field photo shows present day appearance under dense tree canopies (b), slope (c), and corresponding elevation profile of an RCH (d).

studies have focused on the stratigraphy and soil properties of RCHs in the study region (Raab et al. 2017; Hirsch et al. 2017) but the full extent of their distribution and spatial variation throughout the northeast is not known. Iron mining and high concentrations of associated RCHs also occurred in the neighboring states of Massachusetts, New York, and Vermont.

We use LiDAR data as the primary data source in terrain modeling. LiDAR datasets are publically available for the entire states of Connecticut and Massachusetts and parts of New York and Vermont. The LiDAR dataset considered here for northwestern Connecticut was not flown specifically for this study but rather is publicly available on <https://earthexplorer.usgs.gov/>. The dataset was collected under leaf-off conditions in 2011 through the USDA Natural Resources Conservation Service and has an average point spacing of ~2 points per square meter and 1-m pixel resolution in derivative DTMs (Dewberry 2011). Point spacing and resolution are both crucial elements of feature extraction because many archeological landscape features can only be resolved with a resolution of 1 m or better due to their size or shape. RCHs are typically 7–12 m in diameter, but a crucial aspect to their identification is a surrounding ditch or upper/lower lip characterized by locally high slope that is only 1–2 m wide. Such morphology is not visible in datasets that have lower resolutions of 3, 5, or 10 m. Air photos and the most updated land-use and cover information for the study areas was accessed via <http://clear.uconn.edu/>.



Our approach uses the GEOBIA framework. Over the last decade, GEOBIA has been described as the most innovative novel paradigm in modern remote-sensing data processing (Arvor et al. 2013). It has been applied in a wide range of studies ranging from mapping refugees in east Africa (Lang et al. 2010) to documenting penguin guano in Antarctica (Witharana and Lynch 2016), to modeling 3D halite crystals in mud rock samples (Leitner, Peter, and Robert 2014).

GEOBIA attempts to mimic the cognitive processes that humans use in image interpretation, either replicating and/or surpassing the accuracies of expert interpretations via semi- or fully automated workflows (Hay et al. 2005; Blaschke 2010; Marpu et al. 2010). This paradigm has evolved in response to the proliferation of very high-resolution satellite imagery and is now widely acknowledged as an important component of multifaceted RS applications (Jyothi, Babu, and Murali Krishna 2008; Blaschke 2010; Smith and Morton 2010; Kim et al. 2011; Witharana and Civco 2014). GEOBIA involves more than sequential feature extraction (Lang et al. 2008). It furnishes a cohesive methodological platform for machine-based characterization and classification of spatially relevant, real-world entities by using multiscale regionalization techniques augmented with nested representations and rule-based classifiers (Lang et al. 2008; Hagenlocher, Lang, and Tiede 2012).

GEOBIA does not rely on individual pixels but rather pixel groups that are meaningfully cross-pollinated by spectral, textural, geometric, topological, and contextual information. Indeed, one issue in archeological automated extraction techniques has been a lack of contextual information for landscape features, often supplemented by human interpretation (Cowley 2012). From an implementation perspective, GEOBIA is twofold: (1) segmentation and (2) classification. While the former involves creation of image objects using segmentation algorithms, the latter attempts to a semantically map “image” objects to “real-world” objects. Overall, re-segmentation and reclassification provide an expert-based iterative refining model for the classes in question. Our GEOBIA-centered approach to classify RCHs from LiDAR data is shown in Figure 3. This approach attempts to make a meaningful link between low-level image features associated with RCHs encoded in LiDAR-derived terrain models and high-level class labels via multiscale segmentation and knowledge-mounted rulesets.

## 2.2. Data processing

We used ground-classified LiDAR to create 1 m resolution DTMs for candidate study sites. DTMs were then used to produce slope and curvature rasters, which were run through several mathematical morphological operations to better highlight the targets of interest prior to the segmentation process. Use of that method provides additional cues to better operate the segmentation algorithm and yield image segments (image object candidates) with meaningful correspondence to real-world objects. Mathematical morphology (MM) explores the geometric structure of an image in nonlinear fashion (Serra 1982; Dougherty and Lotufo 2003). MM is a well-established image processing framework with its own application merits (Vincent 1994; Soille and Pesaresi 2002; Pesaresi and Benediktsson 2001; Kemper et al. 2011; Pesaresi et al. 2013), however, in this study, we utilized MM operators as preprocessing instruments in the GEOBIA. Erosion and dilation are the most fundamental operations in morphological image processing. While the former erodes the bright areas of the image and expands the dark zones, the latter dilates the bright areas and shrinks the dark areas. Gradient is another MM operator that is useful to find the outline of structures. Based on a series of MM filtering operations, we

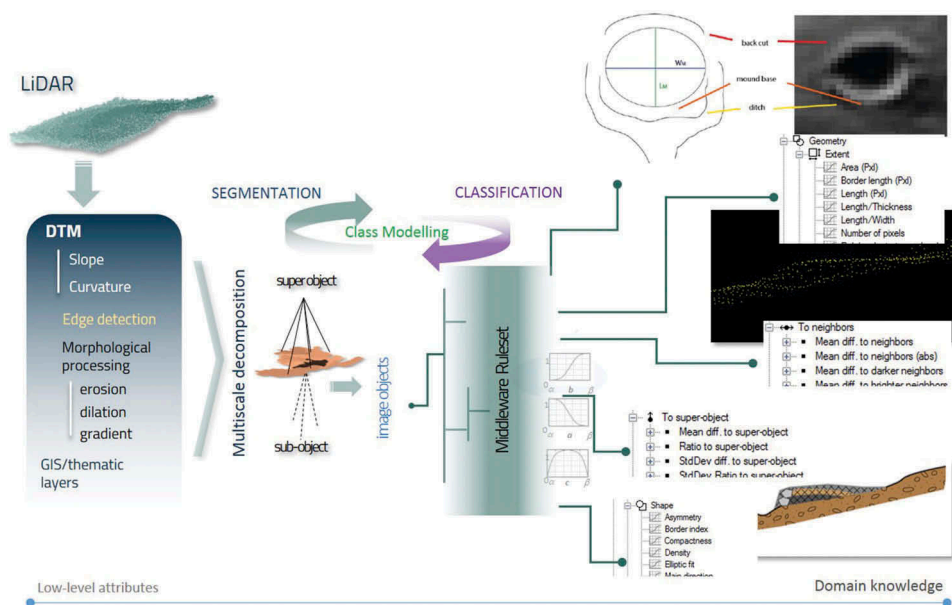


Figure 3. A schematic detailing the conceptual basis of our approach.

selected erosion and gradient as useful operators to create additional rasters from the slope map. We tested a Canny edge detector over the slope raster itself and curvature raster and realized that Canny performs better over the curvature raster.

### 2.3.1. Image segmentation

Image segmentation is the most decisive step in GEOBIA as it paves the way to viable classification results. The key idea of segmentation is to decompose a complex image-scene into nonoverlapping homogeneous regions with nested and scaled representations in scene space (Lang 2008; Kim et al. 2011; Tong et al. 2012; Duro, Franklin, and Dubé 2012). Many segmentation algorithms have been developed and tested over the years. There is no universal algorithm capable of producing perfect segments. There is always a compromise between over-segmentation and under-segmentation. The former is preferred over the latter (Witharana and Civco 2014). Segmentation is an inherently time- and processor-intense procedure. A single-scale segmentation would not suffice since most of the real-world objects and their semantics are embedded into multiple scales. In this study, we utilized three segmentation algorithms: (1) multiresolution segmentation (MRS), (2) contrast-split segmentation, and (3) chessboard segmentation (CBS) (one could view this as a tessellation method than a standard segmentation algorithm), which are available in the eCognition Developer (Trimble Geospatial, Munich) software package. Conceptual basis and methodological implementation of above algorithms are well addressed in literature. While encouraging referring to relevant articles, for the sake of readers' convenience, below we provide short narratives of the candidate segmentation algorithms.

MRS (see Baatz and Schäpe 2000) is a relatively complex and image- and user-dependent algorithm (Hay et al. 2003; Marpu et al. 2010; Witharana and Civco, 201; Grybas, Melendy, and Congalton 2017). The MRS algorithm iteratively merges pixels based on homogeneity criteria driven by three parameters: scale(s), shape, and

compactness (Smith and Morton 2010; Liu et al. 2012; Tong et al. 2012), of which the scale parameter is considered the most important one (Dorren, Maier, and Seijmonsbergen 2003; Smith 2010; Belgiu, Drăguț, and Strobl 2014). Contrast-split segmentation (CSS) is a relatively less-complex and low-performing method compared to the MRS algorithm. CSS is often applied in the image object domain to re-partition image objects belonging to a certain class (i.e., class-specific segmentation). It groups pixels into dark and bright regions (Trimble Germany GmbH 2014). CBS is one of the simplest methods to partition an image into discrete units. It is basically a tessellation method that splits the pixel domain or an image object domain into square image objects. A square grid aligned to the image left and top borders of fixed size is applied to all objects in the domain and each object is cut along these gridlines (Trimble Germany GmbH 2014). This method is frequently used in fine-scale image object operations where one needs to obtain pixel-level segments to use as seed image objects in processes such as image object fusion/growing and boarder optimization.

### 2.3.2. *RCH modeling workflow*

The conceptual basis and the implementation architecture underlying the RCH modeling process is progressively illustrate in Figures 3–5. We first processed LiDAR data to create a DTM and then generated secondary products such as slope, curvature, and Canny edge rasters. Morphological operators, such as erosion, dilation, and gradient, were then run on the secondary products to generate tertiary image layers. For example, the slope raster was subjected to the erosion operator to erode bright areas of the image and expand the dark zones. In the class modeling process (Tiede et al. 2010), the first cycle progressively decomposed the input image layers into meaningful image object candidates and the remaining cycles entailed class/object-specific segmentation. Subsequently, the remote-sensing quantification (low-level image attributes) of image object candidates and domain knowledge on RCHs (Ignatiadis 2016; Raab et al. 2017) was interfaced via a fuzzy rule-based system. We used site-1 to build the master ruleset (Tiede et al. 2010) and later repurposed it with and without adaptations over site-2 to explore the portability of the master ruleset. Figure 4 is a detailed rendition showing how morphologically processed rasters produce image object hierarchy and iteratively refine image object candidates into RCHs. First, the MRS algorithm with large-scale parameter ( $s = 50$ ) was run over the slope raster to produce coarse segments. Basic slope thresholding was then applied to exclude steep and flat segments from further processing with the assumption that RCHs mostly appear on gentle slopes. When segmenting large areas, it is preferred to use large values for the scale parameter as it noticeably reduces the MRS algorithm's processing time and provides more opportunities to repurpose segmentation methods over highly localized image objects (Witharana and Lynch 2016).

After initial segmentation, we re-segmented coarse segments of gentle slope (super objects) based on the erosion raster to small objects (sub-objects) roughly corresponding to the targets of interest. Here, we used the MRS algorithm at the image object level at a fine-scale setting ( $s = 5$ ). This process successfully yielded small seed segments with acceptable correspondence (size and shape) to RCH boundaries. In RCH modeling, based on basic spectral, spatial, and hierarchical criteria, we treated these seed segments as the RCH-like image objects. We identified the immediate neighbors of the RCH-like image objects and re-segmented them based on the contrast-split algorithm and the gradient raster (i.e., secondary processing of erosion raster using the gradient operator). The main idea of this re-segmentation is to frame the sharp edges (front and back of the RCH) in the



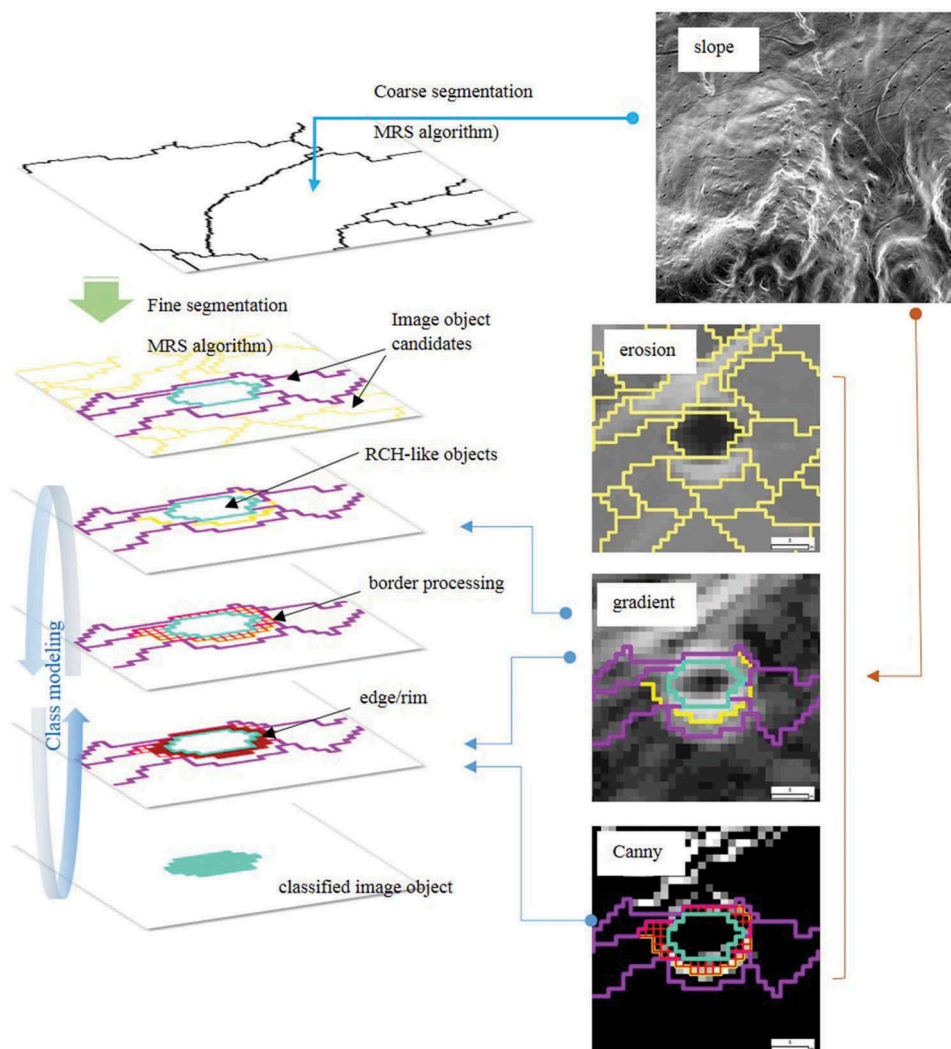


Figure 4. Multiscale segmentation and class modeling of an example RCH.

terrain that have resulted from disturbances (front-cut and back fill) incurred to the natural slope during the construction of charcoal platform (Figures 4 and 5). The sub-objects containing edges were further segmented to the pixel level by using the CBS algorithm. Pixel-level image objects were used as seeds alongside the information from gradient and Canny edge rasters to reconstruct distinct edges (or rims) encircling the RCH-like objects. This step involves object fusion, reshaping, and coating, and other fine-scale object-level operations.

Finally, classification of the RCH is achieved based on the refined RCH-like image object characteristics. Figure 5 illustrates the formulation of the middleware ruleset based on the findings of Johnson and Ouimet (2014), Ignatiadis (2016), and Raab et al. (2017), which provide valuable details about RCHs such as architecture, morphology, original setting, and evolution through time. As seen in the figure, each middleware rule makes a meaningful connection between low-level image attribute(s) and class interpretation. For

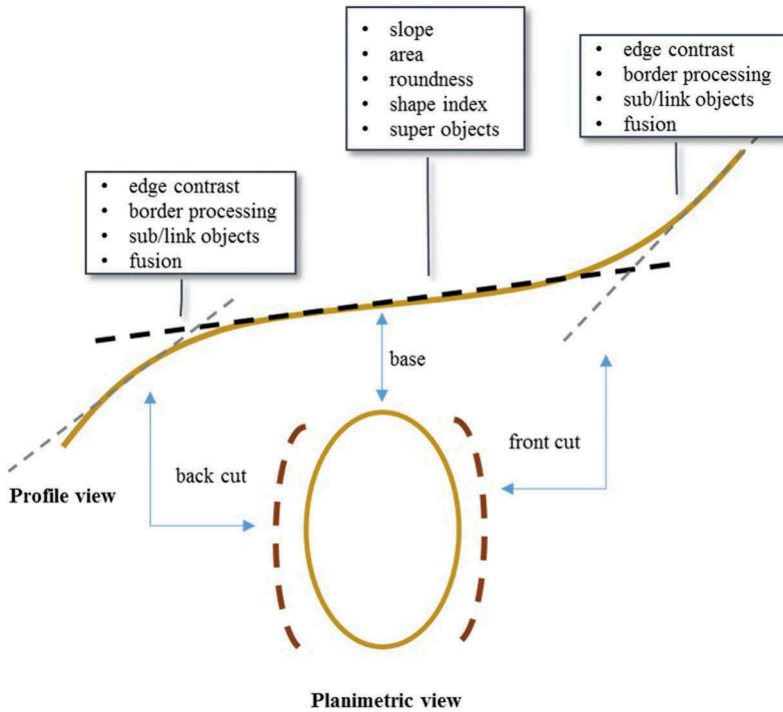


Figure 5. Middleware rules and their connection to the basic anatomy of an example RCH and class modeling.

example, a property such as edge contrast reveals the presence or absence of a back cut or a front cut in the RCH construction (Figure 5). In terms of MRS segmentation, we practiced a quick trial-and-error approach to roughly find optimal values for the scale parameter(s). Our premise was to obtain good (not perfect) segmentation results minimizing under-segmentation and time investments on objective scale-parameter optimization procedures (Witharana and Civco 2014). We assessed the classification actaries of our automated detection based on the manual detection of Johnson, Ouimet, and Raslan (2015) which used a similar LiDAR dataset to that in the present study. We randomly placed  $250 \text{ m} \times 250 \text{ m}$  grid cells in the study areas to sample automated and manual detections. Objective analysis was corroborated with thorough visual inspections to gauge segmentation quality and assess final classification results.

### 2.3.3. Ruleset transferability

While GEOBIA expands the horizon for expert (domain) knowledge integration in fine tuning the classification process, it makes the classification more susceptible for operator-/scene-/target-dependency, which in turn hampers the repeatability and portability of rules (Hofmann et al. 2015; Witharana and Lynch 2016). In this study, we tasked a basic-level analysis of ruleset transferability centered on the framework proposed by Hofmann, Blaschke, and Strobl (2011) for quantifying the robustness of fuzzy rulesets. Use of fuzzy rules (which can take membership values between 0 and 1) is much favored in object-based classification over crisp rules [which can take membership values

constrained to two logical values “true”(=1) and “false”(=0)] because the “fuzzification” of expert-steered thresholds improves transferability. A fuzzy function describing a property  $p$  can be defined using  $\alpha$  (lower border of  $p$ ),  $\beta$  (upper border of  $p$ ),  $a$  (mean of membership function), and  $v$  (range of membership function). We used site-1 to develop the master ruleset (reference ruleset) and applied it over site-2 with and without adaptations to generally gauge the portability of the master ruleset. For the sake of clarity, we briefly describe the relevant robustness measures proposed by Hofmann, Blaschke, and Strobl (2011). More details behind this framework can be found in Hofmann, Blaschke, and Strobl (2011) and Witharana and Lynch (2016). The fuzzy ruleset could undergo three types of changes as Type C, Type O, and Type F, when a reference ruleset ( $R_r$ ) is repurposed as an adapted ruleset ( $R_a$ ) over another image. Type C captures adding, removing, or deactivating a class. Type O is responsible for changing the fuzzy-logic connection of membership functions. Type F involves inclusion or exclusion (Type F<sup>a</sup>) and changing the range of fuzzy membership functions (Type F<sup>b</sup>). The summation of changes yields the total deviations ( $d$ ) incurred during the adaptation of  $R_r$  to  $R_a$  (Hofmann, Blaschke, and Strobl 2011).

$$d = \sum_{i=1}^c C_i + \sum_{i=1}^o O_i + \sum_{i=1}^{f_a} F_i^a + \sum_{i=1}^{f_b} \delta F_i^b$$

$$\delta F = \delta a + \delta v$$

The robustness of the reference ruleset ( $r$ ) can be estimated based on the total deviations ( $d$ ) and classification qualities of reference image ( $q_r$ ) and candidate image ( $q_a$ ) as follows:

$$r_r = \frac{q_a/q_r}{d_a + 1}$$

### 3. Results

Classifying objects such as RCHs in the study region is the result of a sequential process that utilizes different LiDAR-derived products, existing GIS layers, preprocessing methods, segmentation techniques, and domain knowledge (Figure 6). Coarse-scale segmentation based on the slope raster and fine-scale object-specific segmentation produces small image objects that are then classified as RCH-like objects based on basic spectral, spatial, spectral, and super-object characteristics (Figure 6(a)). Figure 6(b) shows how two RCH-like objects (RCH-1 and RCH-2) are strategically refined into true RCH (RCH-1) and false RCH (RCH-2). The presence of edges (based on Canny edge and gradient raster) as semi-circular (lune shaped) objects surrounding RCH-like candidates serves as strong cues on the image object refining process.

In some cases, the manual and automated detection both overlooked actual RCHs (Figure 7). Of the five RCHs (A, B, C, D, E), both manual and automated detection agreed on B, C, D, while the manual detection (Johnson, Ouimet, and Raslan 2015) missed E, and the automated detection missed A. The automated method successfully reconstructed the edges (see yellow arrow) of E; however, it failed to identify a sufficient number of edges in A. It only identified the front-cut of that RCH in the edge images (see magenta arrow). One possible reason the automated detection failed with the Canny edge

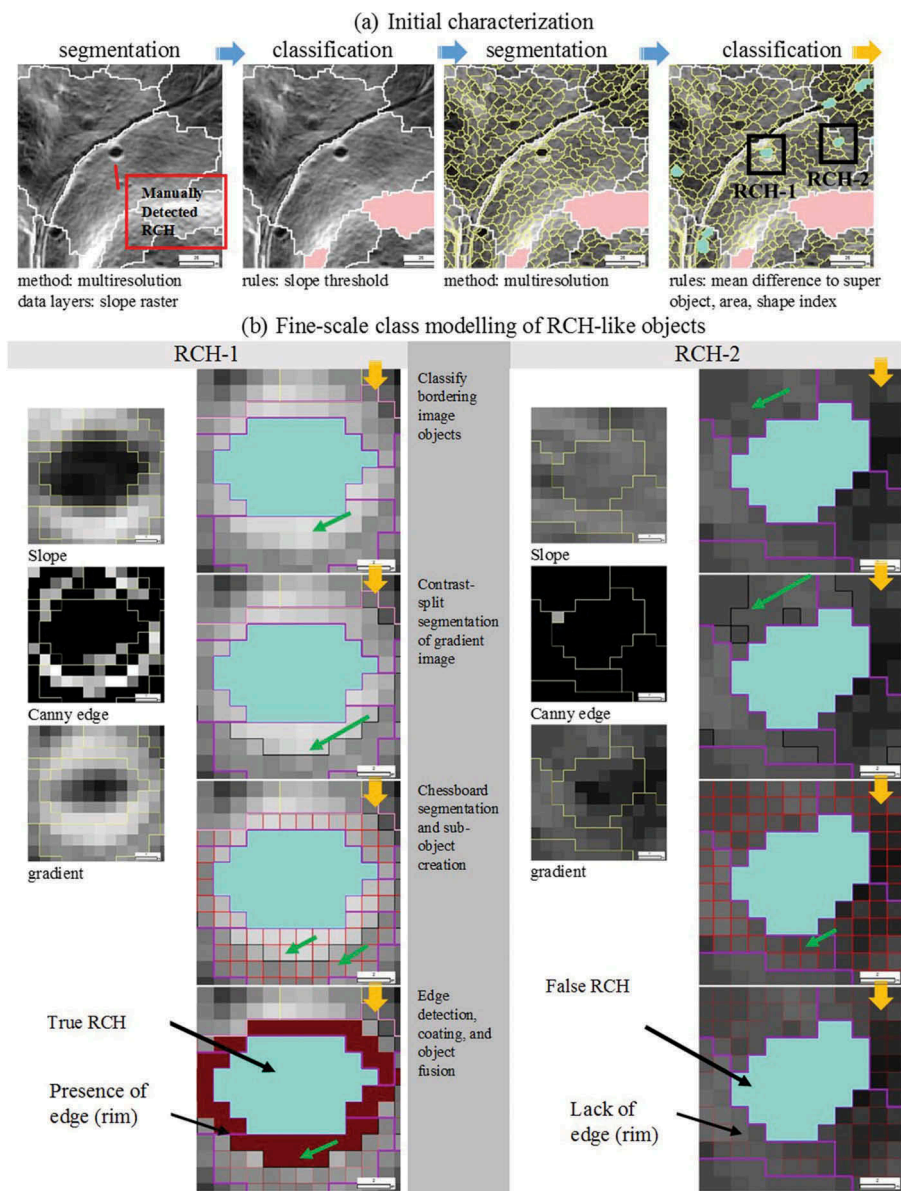


Figure 6. Multiscale modeling of image objects (a) initial identification and (b) fine-scale refining.

detection and gradient rasters here is that there is a gradual slope in the LiDAR profile (see circled area in the downslope) around A. When inspecting the gradient raster (Figure 7(b)) and the Canny edge raster (Figure 7(c)) for E, it is noteworthy how Canny edge detection has overlooked potential edges around E compared with the gradient raster. Overall, the integration of Canny edge detection and gradient provided the necessary filtering to reconstruct a sufficient edge lune around E.

The use of morphological filters played a critical role in the image segmentation process (Figure 8). Figure 8(a) shows three RCH candidates (A, B, C) overlain over the

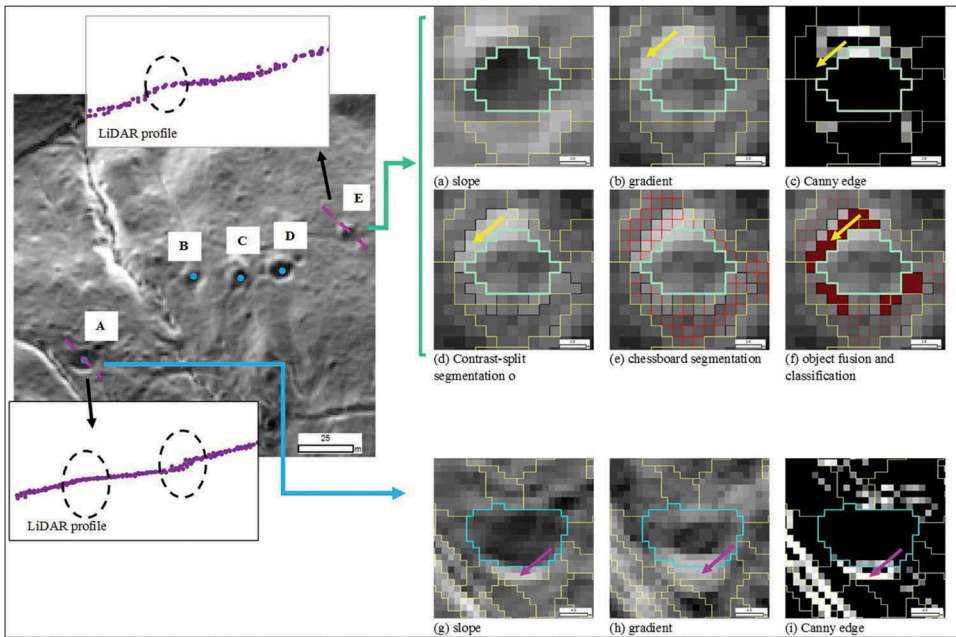


Figure 7. An example disagreement between manual detection and automated detection of RCHs.

slope raster and the morphologically eroded slope raster. Segmentation results based on the slope raster and the eroded slope raster are shown as white and yellow lines, respectively. When inspecting the overlap of these components, it is clear that segmentation based on the erosion raster provides a higher geometrical correspondence to real-world object boundaries than that of the slope raster. This is very clear in rows B and C of Figure 8(a), where segments of the erosion raster elegantly captured the outline of the actual RCH while maintaining the shape and size. Such accurate delineation is critical in proceeding with further classification steps because middleware rules are primarily driven on size, shape, and area characteristics. Improper delineation could lead to misdetection.

In addition to confirming other manually detected features, the automated detection also identified RCHs that manual detection had previously missed (Figure 9). Figure 9 shows classification results for two example grid cells from site-1. While Figure 9(a) shows a perfect agreement between manual and automated detection, Figure 9(b) shows disagreement between two approaches. Zoomed-in views of Figure 9(b) exhibit the discovery of two RCHs, which were actually missed in the reference dataset of Johnson, Ouimet, and Raslan (2015). Also, it reveals a miss detection of the automated approach, perhaps due to the lack of distinct breaks (front cut and back fill) in the slopes. Table 1 reports classification accuracies for site-1 based on the master (reference) ruleset. Based on the randomly sampled grid cells, the automated method recorded user's and producer's accuracies of 73% and 65%, respectively. Table 2 depicts the classification results when the master ruleset repurposed over site-2 as it is (i.e., without adapting fuzzy membership functions). Of the 70 reference RCHs, only 31 RCHs were classified accurate. This leads to a high commission error or very low User's accuracy (44.3%) compared to the Producer's accuracy (75.6%). As seen in Table 3, once the master ruleset is fine tuned to site-2, we were able to achieve a noticeably lower commission error and gained user's and producer's accuracies comparable to those of site-1



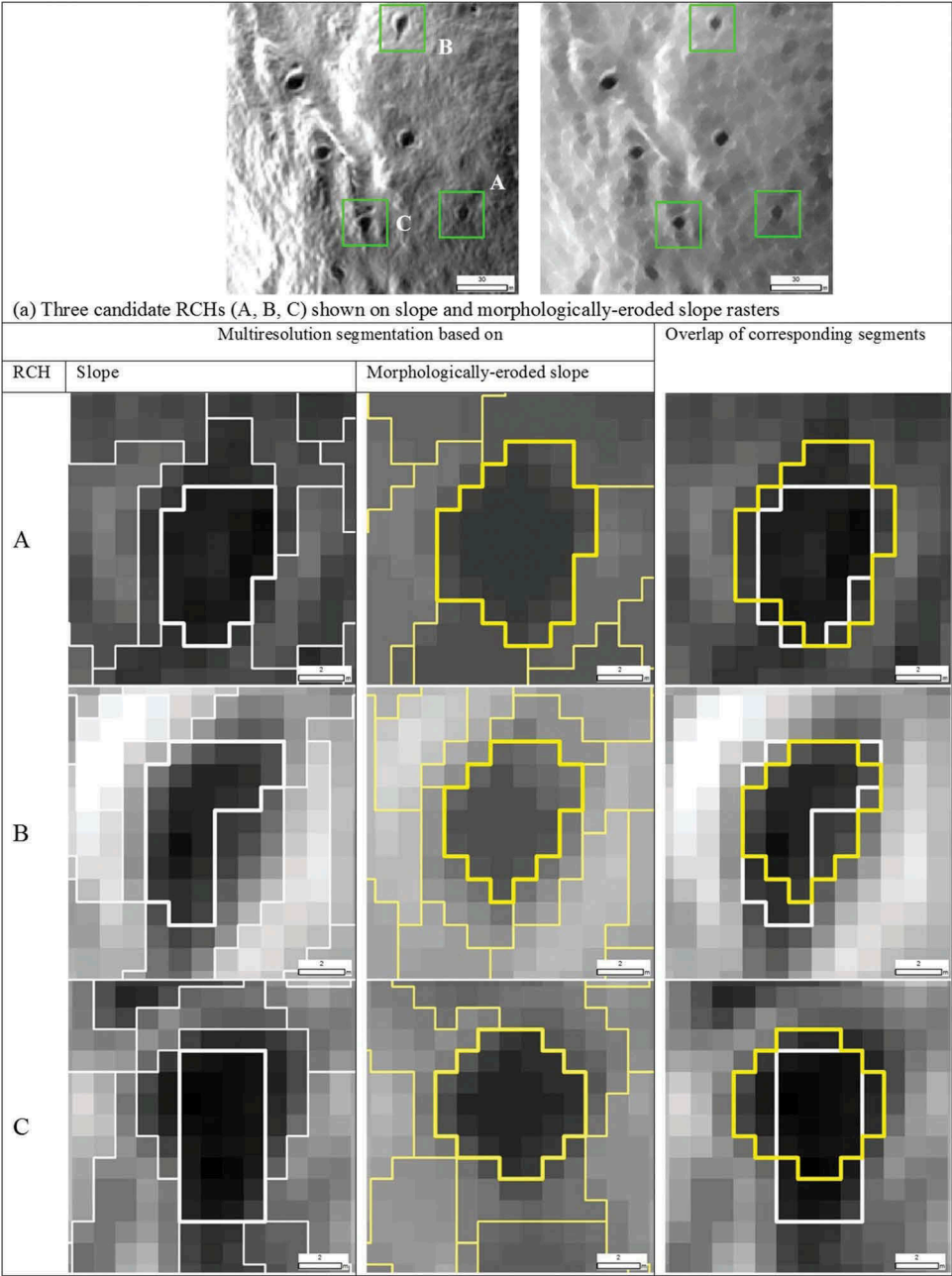


Figure 8. Comparison of segmentation results based on slope raster and morphologically eroded slope raster.

(Table 2). Table 4 reports the key changes made to the reference ruleset during the adaptation. Of the five middleware rules, the slope is the only rule that exhibited a Type  $F^b$  change. Based on the total deviations and classification accuracies, there is a robustness of approximately 0.74.

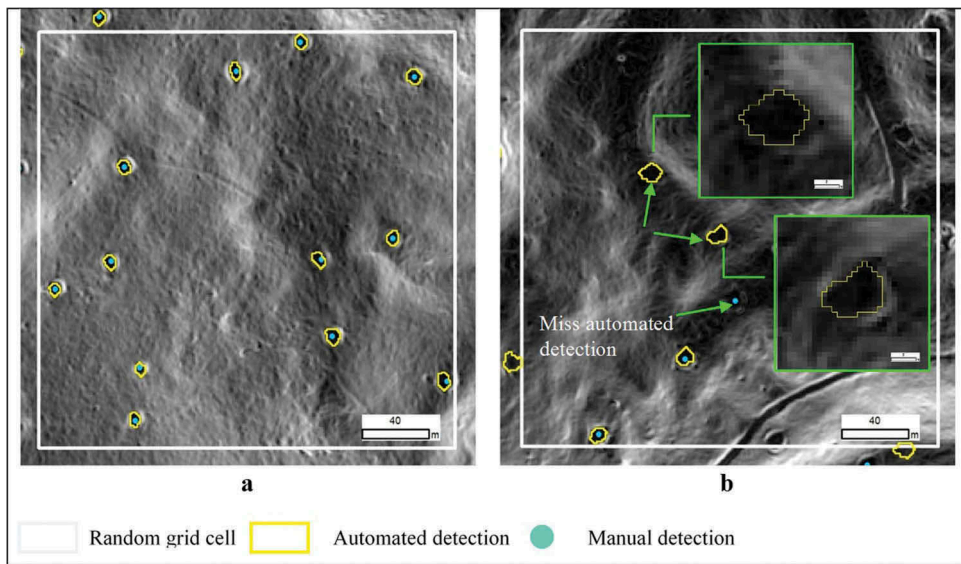


Figure 9. Zoomed-in views of two (a and b) example grid cells from site-1 showing classification results. Figure part (a) shows a perfect agreement between manual (blue) and automated (yellow) detection. Figure part (b) shows disagreement between two approaches. Green insets of figure part (b) exhibit the discovery of two RCHs, which were missed in the reference dataset.

Table 1. Classification accuracies of site-1.

	No. of selected RCHs from random grid cells
Manual detection (based on Johnson, Ouimet, and Raslan 2015)	89
Automatic detection	100
Spatial correspondence between manual and automated detections	65
User's accuracy (%)	73
Producer's accuracy (%)	65

Table 2. Classification accuracies of site-2 based on the master ruleset.

	No. of selected RCHs from random grid cells
Manual detection (based on Johnson, Ouimet, and Raslan 2015)	70
Automatic detection	41
Spatial correspondence between manual and automated detections	31
User's accuracy (%)	44.3
Producer's accuracy (%)	75.6

#### 4. Discussion

The purpose of this study was to explore the potential of GEOBIA using LiDAR data in automated archeological mapping applications. To our knowledge, this is the first GEOBIA-centered effort in RCH mapping from LiDAR-based DTMs as a viable

Table 3. Classification accuracies of site-2 based on the adapted ruleset.

	No. of selected RCHs from random grid cells
Manual detection (based on Johnson, Ouimet, and Raslan 2015)	70
Automatic detection	82
Spatial correspondence between manual and automated detections	50
User's accuracy (%)	71.4
Producer's accuracy (%)	61.0



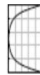


alternative to time- and labor-intense human-augmented image interpretation. Our analysis serves not just as a standard classification workflow but centers on a cohesive conceptual framework, showing the importance of other critical aspects like image preprocessing, class modeling, adaptive segmentation, knowledge base, and transferability of fuzzy rules.

In our analysis, we experimented with and cross-pollinated traditional edge detectors, mathematical morphological operators, complex to simple segmentation methods, and iterative expert-based classification. Rather than relying on standard DTM-based products such as slope, curvature, and hillshade in the workflow, we tested morphological operators such as erosion, dilation, and gradient over slope rasters to better emphasize the features and distill their distinct edges. Such morphologically improved images lead to better segmentation results. As seen on [Figure 8](#), the morphologically filtered slope raster (erosion) produced better quality (good correspondence between the segment and the real-world object) image object candidates than those of the original slope raster. This is because morphological operations such as erosion highlight the boundaries of RCHs, allowing the MRS algorithm to isolate those as homogeneous objects. Some RCHs are poorly defined in the slope raster and blend with the topography. This may be due to insufficient LiDAR point densities, prolonged erosion, or incorporation with other features such as access roads. We found that morphological operations become very handy in highlighting fuzzy RCHs. It is critical to capture the actual morphometry of the object in segmentation because in reality, RCHs have a distinct size and shape; thus, the classification rules ([Figure 5](#)) are primarily governed by the geometrical attributes of the image object candidates. Erroneous boundary delineation during segmentation could potentially place the image object candidates in the wrong class.

Image object candidates that meet the criteria of flat surface, shape, and size do not necessarily guarantee an accurate detection of RCHs. In many instances, the low-level image object attributes could lead to false positives. It is noteworthy that mathematical morphological operators could over-improve natural features as pseudo-RCHs. Therefore, it is necessary to consider other characteristics as well to label a candidate image object as an RCH. When studying the architecture of RCHs and analyzing LiDAR profiles across RCHs, it is clear that an RCH is sandwiched between two breaks in the natural slope ([Figures 1](#) and [5](#)). These distinct slope changes create an edge around the RCH. Depending on the ground conditions and LiDAR point densities, this edge could be continuous, discontinuous, or blended with the surrounding topography. In most instances, two semi-circular (lune shaped) edges could be seen on either side of the RCH ([Figures 6](#) and [7](#)). We identified this feature as an important contextual feature in the refining of RCH-like object candidates ([Figure 6](#)). In order to meaningfully reconstruct the edge, we manipulated pixel-level image objects from Canny edge and gradient images.

Segmentation serves as the precursory step in GEOBIA. Depending on the complexity of the algorithm, segmentation could be a highly time-demanding task. To avoid unnecessary

Table 4. Ruleset adaptation from site-1 to site-2.

Class	Image object property (feature/ variable)	Membership function	Parameters of the master ruleset						Parameters of the adapted ruleset						Deviations			
			$a_r$	$\beta_r$	$v_r$	$a_r$	$a_a$	$\beta_a$	$v_a$	$a_a$	$\delta v$	$\delta a$	$\delta F$	Type F <sup>b</sup>		Type F <sup>a</sup>	Add/Remove/ Change	
RCH-like image objects	Slope		8.0	12.0	4.0	10.0	6.0	10.0	4.0	8.0	0.0	0.3	0.3				–	
	Mean difference to super object		–4.0	–2.0	1.0	–3.0	–4.0	–2.0	1.0	–3.0	0.0	0.0	0.0				–	
	Area		20.0	100.0	80.0	60.0	20.0	100.0	80.0	60.0	0.0	0.0	0.0				–	
	Roundness		0.4	0.6	0.1	0.5	0.4	0.6	0.1	0.5	0.0	0.0	0.0				–	
	Shape index		0.9	1.4	0.5	1.2	0.9	1.4	0.5	1.2	0.0	0.0	0.0				–	



Middleware rules



time investments, we complemented MRS, which is a complex and time intensive method, with the less time-demanding CSS and very simple CBS to produce multi-scale image object candidates. While such hybrid approaches substantially cut down the processing time in large-scale operations, they provide more opportunities to mobilize re-segmentations and reclassification tasks over highly localized image object candidates.

Classification results for site-1 based on the master ruleset are promising. We purposely avoided site-specificity of the master ruleset, i.e., tasking an optimal set of rules. One could gain higher accuracies via the overwhelming number of rules at the expense of poor transferability. Table 1 reveals comparatively higher user's accuracies than producer's accuracies. This may be due to the conservative nature of the master ruleset. More stringent constraints along with more detailed border processing could lower the commission and omission errors. Repurposing the master ruleset on site-2 as it is (Table 2) returned poor classification results. Ideally, we would expect the same level of accuracies for site-2 or better compared to site-1. However, this is not surprising because the terrain characteristics change from site-1 to site-2. It is interesting to see how the classification accuracies (Table 3) improved when the ruleset was adapted. We had to make very few changes to the master ruleset (Table 4). This reflects the degree of adaptability in our middleware rules. However, we emphasize the fact that it is too early to strongly claim the success of our ruleset, especially within the context of transferability. Here, we tested the master ruleset over one study site. To fully understand the transferability, it is necessary to test the master ruleset over a series of sites with varying characteristics. In addition, to address the variability across underlying data, it is important to test the performances of master ruleset over multiple LiDAR datasets (either from multiple acquisitions/modes or synthesizing different point densities from the parent point cloud) with different point densities. In future developments, we will apply this master ruleset over large areas and across LiDAR datasets to see how it performs and explores ways to increase its productivity. As new and higher resolution LiDAR datasets come online for states throughout the northeastern United States where RCHs are found, there may also be new opportunities for improved RCH characterization and refinement of the GEOBIA workflow discussed here.

Undoubtedly, GEOBIA has become a revolutionary framework in modern remote-sensing image processing, as it opens the horizon to integrate domain knowledge via rulesets. However, this fascinating feature itself becomes the main challenge in GEOBIA. Witharana and Lynch (2016) viewed this as GEOBIA's Achilles' heel – the semantic gap (lack of explicit link) – impedes repeatability, transferability, and interoperability of classification workflows. On the one hand, the rule-based classification reduces the semantic gap. On the other hand, it leads to plurality of solutions and hampers the transferability due to the need for significant operator involvement (Hofmann et al. 2015). As a result, it is necessary to pursue alternative directions to meet classification needs. Although mathematical morphological operations were used in image filtering prior to segmentation, we have noticed that those operations work well on slope images. MM is a distinct image processing domain with its own merits. This has been successfully used in gray-scale image processing. Some of the highlighted remote-sensing applications based on high-resolution imagery include damaged building detection (Al-Khudhairi, Caravaggi, and Giada 2005), refugee camp mapping (Kemper et al. 2011), and land-use mapping (Pesaresi et al. 2013). Given the distinct morphology of RCHs, we think that probing a structuring element across morphologically filtered images would be another way to classify RCHs. Thus, in future research, we aim to test MM as a classification tool.



In summary, exploratory studies like ours provide valuable baseline information about best available remote-sensing tools and their opportunities and challenges, not only in targeted automation like RCH characterization but remote-sensing-based mapping of archeological features in a broader context.

## 5. Conclusion

This study explores the potential of object-based image analysis methods to automatically extract RCHs from LiDAR-based DTMs as a viable alternative to time- and labor-intensive human-augmented image interpretation. We combined standard terrain-based rasters, morphological filtering methods, different segmentation algorithms, and knowledge base classification to automatically extract RCHs. We further systematically gauged the classification accuracies and transferability of the object-based rules. Overall, our results are promising. We were able to capture targets of interest with an acceptable accuracy level. We were able to successfully repurpose the main workflow in another area, incurring minimal deviations to the master ruleset.

Datasets generated by this approach provide valuable baseline data for further historical archeological study and understanding of land-use/land-cover change throughout southern New England over the past ~350 years. The analysis, preservation, and conservation of historical features in southern New England are critical. New England is host to one of the densest human populations in the nation, yet heavily forested regions still persist. LiDAR-based mapping and feature extraction allow for datasets of historic features to be created that aid historical preservation efforts and transform conservation and cultural resource management initiatives in the region by enabling scientists, archeologists, and concerned groups to locate, research, catalogue, and demarcate the features, as well as their material sources and impact.

## Disclosure statement

No potential conflict of interest was reported by the authors.

## Funding

This work was supported by National Science Foundation grant: [Grant Number BCS-1654462].

## ORCID

Katharine M. Johnson  <http://orcid.org/0000-0001-7530-762X>

## References

- Al-Khudhairy, D. H. A., I. Caravaggi, and S. Giada. 2005. "Structural Damage Assessments from Ikonos Data Using Change Detection, Object-Oriented Segmentation, and Classification Techniques." *Photogrammetric Engineering & Remote Sensing* 71 (7): 825–837. doi:10.14358/PERS.71.7.825.
- Antonarakis, A. S., K. S. Richards, and J. Brasington. 2008. "Object-Based Land Cover Classification Using Airborne LiDAR." *Remote Sensing of Environment* 112: 2988–2998. doi:10.1016/j.rse.2008.02.004.
- Arvor, D., L. Durieux, S. Andrés, and M.-A. Laporte. 2013. "Advances in Geographic Object-Based Image Analysis with Ontologies: A Review of Main Contributions and Limitations from A

- Remote Sensing Perspective.” *ISPRS Journal of Photogrammetry and Remote Sensing* 82: 125–137. doi:[10.1016/j.isprsjprs.2013.05.003](https://doi.org/10.1016/j.isprsjprs.2013.05.003).
- Baatz, M., and M. Schäpe. 2000. “Multiresolution Segmentation – An Optimization Approach for High Quality Multi-Scale Image Segmentation.” In *Angewandte Geographische Informations-Verarbeitung XIII*, edited by J. Strobl, T. Blaschke, and G. Griesebner, 12–23. Karlsruhe: Wichmann Verlag.
- Belgiu, M., L. Drăguț, and J. Strobl. 2014. “Quantitative Evaluation of Variations in Rule-Based Classifications of Land Cover in Urban Neighbourhoods Using WorldView-2 Imagery.” *ISPRS Journal of Photogrammetry and Remote Sensing* 87 (2014): 205–215. doi:[10.1016/j.isprsjprs.2013.11.007](https://doi.org/10.1016/j.isprsjprs.2013.11.007).
- Bennett, R., K. Welham, R. A. Hill, and A. Ford. 2012. “A Comparison of Visualization Techniques for Models Created from Airborne Laser Scanned Data.” *Archaeological Prospection* 19: 41–48. doi:[10.1002/arp.v19.1](https://doi.org/10.1002/arp.v19.1).
- Blanchard, S. D., M. K. Jakubowski, and M. Kelly. 2011. “Object-Based Image Analysis of Downed Logs in Disturbed Forested Landscapes Using Lidar.” *Remote Sensing* 3: 2420–2439. doi:[10.3390/rs3112420](https://doi.org/10.3390/rs3112420).
- Blaschke, T. 2010. “Object Based Image Analysis for Remote Sensing.” *ISPRS Journal of Photogrammetry and Remote Sensing* 65 (1): 2–16. doi:[10.1016/j.isprsjprs.2009.06.004](https://doi.org/10.1016/j.isprsjprs.2009.06.004).
- Blaschke, T., G. J. Hay, M. Kelly, S. Lang, P. Hofmann, E. Addink, R. Queiroz Feitosa, et al. 2014. “Geographic Object-Based Image Analysis – Towards a New Paradigm.” *ISPRS Journal of Photogrammetry and Remote Sensing* 87 (2014): 180–191. doi:[10.1016/j.isprsjprs.2013.09.014](https://doi.org/10.1016/j.isprsjprs.2013.09.014).
- Challis, K., P. Forlin, and M. Kincey. 2011. “A Generic Toolkit for the Visualization of Archaeological Features on Airborne LiDAR Elevation Data.” *Archaeological Prospection* 18: 279–289. doi:[10.1002/arp.v18.4](https://doi.org/10.1002/arp.v18.4).
- Chase, A. F., D. Z. Chase, J. F. Weishampel, J. B. Drake, R. L. Shrestha, K. C. Slatton, J. J. Awe, and W. E. Carter. 2011. “Airborne LiDAR, Archaeology, and the Ancient Maya Landscape at Caracol, Belize.” *Journal of Archaeological Science* 38: 387–398. doi:[10.1016/j.jas.2010.09.018](https://doi.org/10.1016/j.jas.2010.09.018).
- Chen, G., and G. J. Hay. 2011. “An Airborne Lidar Sampling Strategy to Model Forest Canopy Height from Quickbird Imagery and GEOBIA.” *Remote Sensing of Environment* 115: 1532–1542. doi:[10.1016/j.rse.2011.02.012](https://doi.org/10.1016/j.rse.2011.02.012).
- Cowley, D. C. 2012. “In with the New, Out with the Old? Auto-Extraction for Remote Sensing Archaeology.” In: *Proceedings of SPIE*, edited by C. R. Bostater, S. P. Mertikas, X. Neyt, C. Nichol, D. Cowley, and J.-P. Bruyant, 853206-1–853206-9. Vol. 8532. Edinburgh : SPIE Remote Sensing.
- Crow, P., S. Benham, B. J. Devereux, and G. S. Amable. 2007. “Woodland Vegetation and Its Implications for Archaeological Survey Using LiDAR.” *Forestry* 80: 241–252. doi:[10.1093/forestry/cpm018](https://doi.org/10.1093/forestry/cpm018).
- Dewberry. 2011. “Project Report for the U.S. Corps of Engineers High Resolution LiDAR Data Acquisition and Processing for Portions of Connecticut.” Prepared for USDA-NRCS, September 2011.
- Doneus, M., C. Briese, M. Fera, and M. Janner. 2008. “Archaeological Prospection of Forested Areas Using Full-Waveform Airborne Laser Scanning.” *Journal of Archaeological Science* 35: 882–893. doi:[10.1016/j.jas.2007.06.013](https://doi.org/10.1016/j.jas.2007.06.013).
- Dorren, L. K. A., B. Maier, and A. C. Seijmonsbergen. 2003. “Improved Landsat-Based Forest Mapping in Steep Mountainous Terrain Using Object-Based Classification.” *Forest Ecology and Management* 183 (1–3): 31–46. doi:[10.1016/S0378-1127\(03\)00113-0](https://doi.org/10.1016/S0378-1127(03)00113-0).
- Dougherty, E. R., and R. A. Lotufo. 2003. *Hands on Morphological Image Processing*, 272. Bellingham: SPIE Press.
- Duro, D. C., S. E. Franklin, and M. G. Dubé. 2012. “A Comparison of Pixel-Based and Object-Based Image Analysis with Selected Machine Learning Algorithms for the Classification of Agricultural Landscapes Using SPOT-5 HRG Imagery.” *Remote Sensing of Environment* 118 (2012): 259–272. doi:[10.1016/j.rse.2011.11.020](https://doi.org/10.1016/j.rse.2011.11.020).
- Evans, D. H., R. J. Fletcher, C. Pottier, J.-B. Chevance, D. Soutif, B. S. Tan, S. Im, et al. 2013. “Uncovering Archaeological Landscapes at Angkor Using Lidar.” *Proceedings of the National Academy of Sciences* 110: 12595–12600. doi:[10.1073/pnas.1306539110](https://doi.org/10.1073/pnas.1306539110).
- Foster, D. R., B. Donahue, D. Kittredge, G. Motzkin, B. Hall, B. Turner, and E. Chilton. 2008. “New England’s Forest Landscape: Ecological Legacies and Conservation Patterns Shaped by

- Agrarian History.” In: *Agrarian Landscapes in Transition: Comparisons of Long-Term Ecological & Cultural Change*, edited by C. R. Redman and D. R. Foster, 44–88. New York: Oxford University Press.
- Gallagher, J. M., and R. L. Josephs. 2008. “Using LiDAR to Detect Cultural Resources in a Forested Environment: An Example from Isle Royale National Park, Michigan, USA.” *Archaeological Prospection* 15: 187–206. doi:[10.1002/arp.v15i3](https://doi.org/10.1002/arp.v15i3).
- Grybas, H., L. Melendy, and R. G. Congalton. 2017. “A Comparison of Unsupervised Segmentation Parameter Optimization Approaches Using Moderate- and High-Resolution Imagery.” *GIScience & Remote Sensing* 54 (4): 515–533. doi:[10.1080/15481603.2017.1287238](https://doi.org/10.1080/15481603.2017.1287238).
- Gu, H., H. Li, L. Yan, Z. Liu, T. Blaschke, and U. Soergel. 2017. “An Object-Based Semantic Classification Method for High Resolution Remote Sensing Imagery Using Ontology.” *Remote Sensing* 9 (4): 329. doi:[10.3390/rs9040329](https://doi.org/10.3390/rs9040329).
- Hagenlocher, M., S. Lang, and D. Tiede. 2012. “Integrated Assessment of the Environmental Impact of an IDP Camp in Sudan Based on Very High Resolution Multi-Temporal Satellite Imagery.” *Remote Sensing of Environment* 126: 27–38. doi:[10.1016/j.rse.2012.08.010](https://doi.org/10.1016/j.rse.2012.08.010).
- Hay, G. J., G. Castilla, M. A. Wulder, and J. R. Ruiz. 2005. “An Automated Object-Based Approach for the Multiscale Image Segmentation of Forest Scenes.” *International Journal of Applied Earth Observation and Geoinformation* 7 (4): 339–359. doi:[10.1016/j.jag.2005.06.005](https://doi.org/10.1016/j.jag.2005.06.005).
- Hay, G. J., T. Blaschke, D. J. Marceau, and A. Bouchard. 2003. “A Comparison of Three Image-Object Methods for the Multiscale Analysis of Landscape Structure.” *ISPRS Journal of Photogrammetry and Remote Sensing* 57 (5–6): 327–345. doi:[10.1016/S0924-2716\(02\)00162-4](https://doi.org/10.1016/S0924-2716(02)00162-4).
- Hesse, R. 2010. “LiDAR-derived Local Relief Models – A New Tool for Archaeological Prospection.” *Archaeological Prospection* 17: 67–72.
- Hirsch, F., T. Raab, W. Ouimet, D. Dethier, A. Schneider, and A. Raab. 2017. “Soils on Historic Charcoal Hearths: Terminology and Chemical Properties.” *Soil Science Society of America Journal* 81: 1427. doi:[10.2136/sssaj2017.02.0067](https://doi.org/10.2136/sssaj2017.02.0067).
- Hofmann, P., P. Lettmayer, T. Blaschke, M. Belgiu, S. Wegenkittl, R. Graf, T. J. Lampoltshammer, and V. Andrejchenko. 2015. “Towards a Framework for Agent-Based Image Analysis of Remote-Sensing Data.” *International Journal of Image and Data Fusion* 6 (2): 115–137. doi:[10.1080/19479832.2015.1015459](https://doi.org/10.1080/19479832.2015.1015459).
- Hofmann, P., T. Blaschke, and J. Strobl. 2011. “Quantifying the Robustness of Fuzzy Rule Sets in Object-Based Image Analysis.” *International Journal of Remote Sensing* 32 (22): 7359–7381. doi:[10.1080/01431161.2010.523727](https://doi.org/10.1080/01431161.2010.523727).
- Howey, M. C. L., F. B. Sullivan, J. Tallant, R. Vande Kopple, and M. W. Palace. 2016. “Detecting Precontact Anthropogenic Microtopographic Features in A Forested Landscape with Lidar: A Case Study from the Upper Great Lakes Region, AD 1000–1600.” *PLoS One* 11: 1–11. doi:[10.1371/journal.pone.0162062](https://doi.org/10.1371/journal.pone.0162062).
- Ignatiadis, M. E. 2016. *Charcoal-Rich Mounds in Litchfield County CT Record Widespread Hillslope Disturbance in the Iron Corridor from Mid 18th to Early 20th Centuries*. Williamstown: Williams College.
- Johnson, K. M., and W. B. Ouimet. 2014. “Rediscovering the Lost Archaeological Landscape of Southern New England Using Airborne Light Detection and Ranging (Lidar).” *Journal of Archaeological Science* 43: 9–20. doi:[10.1016/j.jas.2013.12.004](https://doi.org/10.1016/j.jas.2013.12.004).
- Johnson, K. M., and W. B. Ouimet. 2016. “Physical Properties and Spatial Controls of Stone Walls in the Northeastern USA: Implications for Anthropocene Studies of 17th to Early 20th Century Agriculture.” *Anthropocene* 15: 22–36. doi:[10.1016/j.ancene.2016.07.001](https://doi.org/10.1016/j.ancene.2016.07.001).
- Johnson, K. M., W. B. Ouimet, and Z. Raslan. 2015. “Geospatial and LiDAR-based Analysis of 18th to Early 20th Century Timber Harvesting and Charcoal Production in Southern New England.” *Geological Society of America Abstracts with Programs* 47: 65.
- Jyothis, B. N., G. R. Babu, and L. V. Murali Krishna. 2008. “Object Oriented and Multi-Scale Image Analysis: Strengths, Weaknesses, Opportunities and Threats-A Review.” *Journal of Computer Science* 4 (9): 706–712. doi:[10.3844/jcssp.2008.706.712](https://doi.org/10.3844/jcssp.2008.706.712).
- Kemper, T., M. Jenerowicz, M. Pesaresi, and P. Soille. 2011. “Enumeration of Dwellings in Darfur Camps from GeoEye-1 Satellite Images Using Mathematical Morphology.” *IEEE Journal of Selected Topics in Applied Earth Observations and Remote Sensing* 4 (1): 8–15. doi:[10.1109/JSTARS.2010.2053700](https://doi.org/10.1109/JSTARS.2010.2053700).
- Kim, M., T. A. Warner, M. Madden, and D. S. Atkinson. 2011. “Multi-Scale GEOBIA with Very High Spatial Resolution Digital Aerial Imagery: Scale, Texture and Image Objects.”

- International Journal of Remote Sensing* 32 (10): 2825–2850. doi:10.1080/01431161003745608.
- Kokalj, Ž., K. Zakšek, and K. Oštir. 2011. “Application of Sky-View Factor for the Visualisation of Historic Landscape Features in Lidar-Derived Relief Models.” *Antiquity* 85: 263–273. doi:10.1017/S0003598X00067594.
- Lang, S. 2008. Object-based image analysis for remote sensing applications: Modeling reality—Dealing with complexity. In *Object-Based Image Analysis*; Blaschke, T., Lang, S., Geoffrey, H., Eds.; Springer: Heidelberg, Germany; Berlin, Germany; New York, NY, USA.
- Lang, S., D. Tiede, D. Hölbling, P. Füreder, and P. Zeil. 2010. “Earth Observation (Eo)-Based Ex Post Assessment of Internally Displaced Person (IDP) Camp Evolution and Population Dynamics in Zam Zam, Darfur.” *International Journal of Remote Sensing* 31 (21): 5709–5731. doi:10.1080/01431161.2010.496803.
- Lang, S. 2008. “Object-Based Image Analysis for Remote Sensing Applications: Modeling Reality – Dealing with Complexity.” In: *Object-Based Image Analysis*, edited by T. Blaschke, S. Lang, and G. Hay. Heidelberg: Springer.
- Lasaponara, R., and N. Masini. 2009. “Full-Waveform Airborne Laser Scanning for the Detection of Medieval Archaeological Microtopographic Relief.” *Journal of Cultural Heritage* 10: e78–e82. doi:10.1016/j.culher.2009.10.004.
- Leitner, C., H. Peter, and M. Robert. 2014. “3d-Modeling of Deformed Halite Hopper Crystals by Object Based Image Analysis.” *Computers & Geosciences* 73 (C): 61–70. doi:10.1016/j.cageo.2014.08.010.
- Liu, Y., L. Bian, Y. Meng, H. Wang, S. Zhang, Y. Yang, X. Shao, and B. Wang. 2012. “Discrepancy Measures for Selecting Optimal Combination of Parameter Values in Object-Based Image Analysis.” *ISPRS Journal of Photogrammetry and Remote Sensing* 68 (2012): 144–156. doi:10.1016/j.isprsjprs.2012.01.007.
- Luo, L., X. Wang, H. Guo, C. Liu, J. Liu, L. Li, X. Du, and G. Qian. 2014. “Automated Extraction of the Archaeological Tops of Qanat Shafts from VHR Imagery in Google Earth.” *Remote Sensing* 6: 11956–11976. doi:10.3390/rs61211956.
- Marpu, P. R., M. Neubert, H. Herold, and I. Niemeyer. 2010. “Enhanced Evaluation of Image Segmentation Results.” *Journal of Spatial Science* 55 (1): 55–68. doi:10.1080/14498596.2010.487850.
- McCoy, M. D., G. P. Asner, and M. W. Graves. 2011. “Airborne Lidar Survey of Irrigated Agricultural Landscapes: An Application of the Slope Contrast Method.” *Journal of Archaeological Science* 38: 2141–2154. doi:10.1016/j.jas.2011.02.033.
- Millard, K., C. Burke, D. Stiff, and A. Redden. 2009. “Detection of a Low-Relief 18th-Century British Siege Trench Using LiDAR Vegetation Penetration Capabilities at Fort Beauséjour-Fort Cumberland National Historic Site, Canada.” *Geoarchaeology* 24: 576–588. doi:10.1002/gea.v24:5.
- Opitz, R. S., K. Ryzewski, J. F. Cherry, and B. Moloney. 2015. “Using Airborne LiDAR Survey to Explore Historic-Era Archaeological Landscapes of Montserrat in the Eastern Caribbean.” *Journal of Field Archaeology* 40: 523–541. doi:10.1179/2042458215Y.0000000016.
- Pesaresi, M., G. Huadong, X. Blaes, D. Ehrlich, S. Ferri, L. Gueguen, M. Halkia, et al. 2013. “A Global Human Settlement Layer from Optical HR/VHR RS Data: Concept and First Results.” *IEEE Journal of Selected Topics in Applied Earth Observations and Remote Sensing* 6 (5): 2102–2131. doi:10.1109/JSTARS.2013.2271445.
- Pesaresi, M., and J. A. Benediktsson. 2001. “A New Approach for the Morphological Segmentation of High-Resolution Satellite Imagery.” *IEEE Transactions on Geoscience and Remote Sensing* 39 (2): 309–320. doi:10.1109/36.905239.
- Prüfer, K., and A. E. Thompson. 2016. “Lidar-Based Analyses of Anthropogenic Landscape Alterations as a Component of the Built Environment.” *Advances in Archaeological Practice* 4: 393–409. doi:10.7183/2326-3768.4.3.393.
- Raab, T., F. Hirsch, W. Ouimet, K. Johnson, D. Dethier, and A. Raab. 2017. “Architecture of Relict Charcoal Hearths in Northwestern Connecticut, USA.” *Geoarchaeology* 32 (4): 502–510. doi:10.1002/gea.21614.
- Randall, A. R. 2014. “LiDAR-aided Reconnaissance and Reconstruction of Lost Landscapes: An Example of Freshwater Shell Mounds (Ca. 7500–500 Cal B.P.) in Northeastern Florida.” *Journal of Field Archaeology* 39: 162–179. doi:10.1179/0093469014Z.00000000080.

- Schneider, A., M. Takla, A. Nicolay, A. Raab, and T. Raab. 2015. "A Template-Matching Approach Combining Morphometric Variables for Automated Mapping of Charcoal Kiln Sites." *Archaeological Prospection* 22: 45–62. doi:10.1002/arp.v22.1.
- Serra, J. 1982. *Image Analysis and Mathematical Morphology*, 621. London: Academic Press.
- Smith, A. 2010. "Image Segmentation Scale Parameter Optimization and Land Cover Classification Using the Random Forest Algorithm." *Journal of Spatial Science* 55 (1): 69–79. doi:10.1080/14498596.2010.487851.
- Smith, G. M., and R. D. Morton. 2010. "Real World Objects in GEOBIA through the Exploitation of Existing Digital Cartography and Image Segmentation." *Photogrammetric Engineering & Remote Sensing* 76 (2): 163–171. doi:10.14358/PERS.76.2.163.
- Smits, I., G. Frieditis, S. Dagis, and D. Dubrovskis. 2012. "Individual Tree Identification Using Different LIDAR and Optical Imagery Data Processing Methods." *Biosystems and Information Technology* 1: 19–24.
- Soille, P., and M. Pesaresi. 2002. "Advances in Mathematical Morphology Applied to Geoscience and Remote Sensing." *IEEE Transactions on Geoscience and Remote Sensing* 40 (9): 2042–2055. doi:10.1109/TGRS.2002.804618.
- Tiede, D., S. Lang, D. Höbling, and P. Füreder. 2010. "Transferability of OBIA Rulesets for IDP Camp Analysis in Darfur." In: *GEOBIA*, edited by E. A. Addink and F. M. B. van Coillie. Vol. XXXVIII-4/C7. Archives ISSN No 1682-1777. ISPRS. Ghent: Ghent University.
- Tong, H., T. Maxwell, Y. Zhang, and V. A. Dey. 2012. "A Supervised and Fuzzy-Based Approach to Determine Optimal Multi-Resolution Image Segmentation Parameters." *Photogrammetric Engineering & Remote Sensing* 78 (10): 1029–1044. doi:10.14358/PERS.78.10.1029.
- Trier, Ø. D., and L. H. Pilø. 2012. "Automatic Detection of Pit Structures in Airborne Laser Scanning Data." *Archaeological Prospection* 19: 103–121. doi:10.1002/arp.v19.2.
- Trier, Ø. D., M. Zortea, and C. Tønning. 2015. "Automatic Detection of Mound Structures in Airborne Laser Scanning Data." *Journal of Archaeological Science: Reports* 2: 69–79. doi:10.1016/j.jasrep.2015.01.005.
- Trier, Ø. D., S. Ø. Larsen, and R. Solberg. 2009. "Automatic Detection of Circular Structures in High-Resolution Satellite Images of Agricultural Land." *Archaeological Prospection* 16: 1–15. doi:10.1002/arp.v16.1.
- Trimble Germany GmbH. 2014. *eCognition Developer 8.7.2 Reference Book*. Germany: Trimble Germany GmbH.
- Verhagen, P., and L. Drăguț. 2012. "Object-Based Landform Delineation and Classification from DEMs for Archaeological Predictive Mapping." *Journal of Archaeological Science* 39 (3): 698–703. doi:10.1016/j.jas.2011.11.001.
- Vincent, L. 1994. "Morphological Area Openings and Closings for Grey-Scale Images." In: *Shape in Picture: Mathematical Description of Shape in Grey-Level Images*, edited by O. Ying-Lie, A. Toet, D. Foster, H. J. A. M. Heijmans, and P. Meer, 197–208. Berlin: Springer Berlin Heidelberg.
- Witharana, C., and D. L. Civco. 2014. "Optimizing Multi-Resolution Segmentation Scale Using Empirical Methods: Exploring the Sensitivity of the Supervised Discrepancy Measure Euclidean Distance 2 (ED2)." *ISPRS Journal of Photogrammetry and Remote Sensing* 87: 108–121. doi:10.1016/j.isprsjprs.2013.11.006.
- Witharana, C., and H. Lynch. 2016. "An Object-Based Image Analysis Approach for Detecting Penguin Guano in Very High Spatial Resolution Satellite Images." *Remote Sensing* 8 (5): 375. doi:10.3390/rs8050375.